ADAPTIVE REGULARIZATION LEVEL SET EVOLUTION FOR MEDICAL IMAGE SEGMENTATION AND BIAS FIELD CORRECTION

Xiaomeng Xin[1,2]*, Lingfeng Wang*[1]*, Chunhong Pan*[1] *and Shigang Liu*[2]

1. NLPR, Institute of Automation, Chinese Academy of Sciences
2. School of Computer Science, Shaanxi Normal University

ABSTRACT

In this paper, we propose a level-set based segmentation method for medical images with intensity inhomogeneity. Maximum a Posteriori estimation is adopted to combine image segmentation and bias field correction into a unified framework. Within this framework, both contour prior and bias field prior can be fully used. In order to restrict bias field, we introduce an adaptive regularization. Based on this new adaptive regularization, the bias field is estimated more smooth and the input medical image with intensity inhomogeneity is recovered more clearly. Especially, the estimated bias field of our method introduces less structure information obtained from input image. Experimental results on both synthetic and real images show the advantages of our method in both segmentation and bias field correction accuracies as compared with the state-of-the-art approaches.

***Index Terms*—** Level set, adaptive regularization, image segmentation, bias field

1. INTRODUCTION

Image segmentation is a key component in various medical imaging systems [1–3]. It is a fundamental step for subsequent tasks, such as 3D reconstruction and object recognition. In many medical imaging systems, the output medical images often present intensity inhomogeneity caused by bias field. Hence, it is important to develop some algorithms that can segment the images with intensity inhomogeneity, or simultaneously segment images and correct the bias field [4, 5].

In recent years, numerous approaches have been proposed for medical image segmentation simultaneous with bias field correction. Li et al. [6] developed an approach based on local image mean for interleaved bias field estimation and segmentation. However, the computational cost of this model is a bit high due to the utilization of local models, which involves many convolution operations on images. Motivated by Li's method, Zhang et al. [7] considered both local image variance and mean in a multi-phase level set approach, which has many advantages such as the evolution is less sensitive to the initialization. whereas the estimated bias field in this approach contains too much structural information of the original image. Wang et al. [8] introduced a fixed regularization to smooth the bias field. This method assumes that bias field and reciprocal bias field both vary slowly in the entire image. In [9], Li et al. utilized a linear combination of a number of smooth basis functions to approximate the bias field. Improved performances compared with the classical methods have been reported in these papers. However, these methods compute the bias field roughly by fixed smoothing operators, such as the Gaussian kernel and gradient operator.

Motivated by previous work [6,8], we propose an effective level-set based segmentation method. In our method, the segmentation and bias field correction problems are formulated simultaneously by a variational energy functional.

Specifically, the main advantages and contributions of our work are highlighted as follows:

1. Maximum a posteriori estimation method is utilized to unify segmentation and bias field correction into a uniform framework. Therefore, our model can make full use of the prior knowledge on the segmented contour and the bias field.

2. An adaptive regularization is introduced to restrict the spatial smoothness of the bias field. Due to the adaptive regularization, the estimated bias field of our method is more smooth and has less structural information of the original image. Especially, for an image with weak edges and strong biased regions, the segmentation results of our method are better than the state-of-the-art approaches.

2. METHODOLOGY

2.1. Bayesian Framework

We consider the following model to formulate medical image formation with multiplicative bias field:

$$I(\mathbf{x}) = b(\mathbf{x})J(\mathbf{x}) + n(\mathbf{x}) \ , \quad \mathbf{x} \in \Omega \ , \tag{1}$$

where I is the input image, Ω is the two dimensional image domain, J is the true image, b is the bias field, and n is the additive Gaussian white noise. The purpose of image segmentation is to find a segmentation contour $\mathcal{C}$, while the goal of bias correction is to directly estimate the bias field b from the observed image I. In our work, the above two tasks are considered together, and further unified as a Bayesian estimation problem

$$\mathcal{C}^\star, b^\star = \arg\max \ p(\mathcal{C}, b|I) \ . \tag{2}$$

Based on the Bayes' theorem, Eqn. (2) can be reformulated as

$$\begin{aligned} \mathcal{C}^\star, b^\star &= \arg\max \ p(\mathcal{C}, b|I) \\ &\propto \arg\max \ p(I|\mathcal{C}, b)p(\mathcal{C})p(b) \ , \end{aligned} \tag{3}$$

where the bias field b and $\mathcal{C}$ are assumed to be independent. Maximum a posteriori estimation in Eqn. (3) is equivalent to minimizing the following objective functional

$$\mathcal{F}(\mathcal{C}, b) = \mathcal{L}(I|\mathcal{C}, b) + \nu\mathcal{R}(\mathcal{C}) + \mu\mathcal{A}(b) \ , \tag{4}$$

This work is supported by the National Natural Science Foundation of China under Grants 61403376, 61175025 and 61402274.

where ν and μ are two positive weighting parameters used to balance the likelihood and two priors. The term $\mathcal{L}(I|\mathcal{C},b)$ is the segmentation likelihood presented in Subsection 2.2, $\mathcal{R}(\mathcal{C})$ is contour prior described in Subsection 2.3, and $\mathcal{A}(b)$ is adaptive bias field prior introduced in Subsection 2.4.

2.2. Segmentation Likelihood

As with the previous work [8, 9], the recovered true image J is assumed to be composed of N disjoint regions, satisfying that

$$\Omega = \bigcup_{i=1}^{N} \Omega_i \ , \Omega_i \cap \Omega_j = \emptyset \ , \forall\, 1 \leq i \neq j \leq N \ . \tag{5}$$

The intensity value in the i-th region is approximate to a constant c_i, namely,

$$J(\mathbf{x}) \approx c_i \ , \mathbf{x} \in \Omega_i \ . \tag{6}$$

Combining with Eqn. (1), $b(\mathbf{x})c_i \ , (\mathbf{x} \in \Omega_i)$ can be regarded as the intensity value in the i-th region in the observed image, that is,

$$I(\mathbf{x}) \approx b(\mathbf{x})c_i \ , \mathbf{x} \in \Omega_i \ . \tag{7}$$

Based on Eqn. (7), the segmentation likelihood energy $\mathcal{L}(I|\mathcal{C},b)$ is

$$\mathcal{L}(I|\mathcal{C},b) = \sum_{i=1}^{N} \left(\gamma_i \int_{\mathbf{x}\in\Omega_i} (I(\mathbf{x}) - b(\mathbf{x})c_i)^2 \mathrm{d}\mathbf{x} \right) \ , \tag{8}$$

where γ_i is the positive constant for the i-th region.

2.3. Contour Prior

In this work, we do not have any special knowledge on the segmented objects. Hence, it is hard to introduce shape priors [10, 11] on the segmentation contour. Therefore, the contour length prior is used to represent contour prior energy, given by

$$\mathcal{R}(\mathcal{C}) = |\mathcal{C}| \ , \tag{9}$$

where $|\mathcal{C}|$ represents the length of the contour $\mathcal{C}$.

2.4. Adaptive Bias Field Regularization

In contrast to the traditional regularization proposed in [8], which specifies a fixed regularization operator to penalize the bias field, we estimate it simultaneously with parameters. We assume that the prior distribution $p(b)$ is unknown, but is close to the model distribution $q(b)$ in terms of Kullback-Leibler (KL) divergence. Accordingly, the adaptive bias field regularization in Eqn. (4) is represented as

$$\mathcal{A}(b) = \mathcal{S}(b) + \mathcal{KL}(p(b)||q(b)) \ , \tag{10}$$

where $\mathcal{S}(b) = \log(p(b))$ is the smooth regularization used to restrict that the bias field b should be spatially smooth, and $\mathcal{KL}(p(b)||q(b))$ is the KL-divergence between the unknown prior distribution $p(b)$ and the model distribution $q(b)$. In this work, the two distributions $p(b)$ and $q(b)$ are assumed to be zero-mean multivariate Gaussian distribution with covariances Σ and Ω respectively, that is,

$$p(b) \sim N(0, \Sigma) \ , q(b) \sim N(0, \Omega) \ . \tag{11}$$

Hence, Eqn. (10) can be reformulated as

$$\mathcal{A}(b) = \frac{1}{2} b^T \Sigma^{-1} b + \frac{1}{2} \mathrm{tr}(\Omega^{-1}\Sigma) + \mathrm{const} \ , \tag{12}$$

where $\mathrm{tr}(\cdot)$ is the trace of the matrix. Motivated by the analysis presented in [12], the covariances Σ and Ω are assumed to be

$$\Sigma^{-1} = Q\Lambda Q^T \ , \Omega^{-1} = QKQ^T \ , \tag{13}$$

where $\Lambda = \mathrm{diag}[\lambda_1, \lambda_2, \ldots, \lambda_M]$, $K = \mathrm{diag}[k_1, k_2, \ldots, k_M]$ and $Q = [q_1, q_2, \ldots, q_M]$ is a Discrete Cosine Transform (DCT) basis. Hence, Eqn. (10) can be reformulated as

$$\mathcal{A}(b) = \frac{1}{2} \sum\nolimits_{i=1}^{M} \lambda_i (q_i^T b)^2 + \frac{1}{2} \sum\nolimits_{i=1}^{M} \frac{k_i}{\lambda_i} \ . \tag{14}$$

By solving variables $\{\lambda_i\}_{i=1}^M$ from Eqn. (14), we get

$$\lambda_i = \frac{\sqrt{k_i}}{|q_i^T b|} \ , \forall i = 1, 2, \cdots, M \ .$$

Substituting $\{\lambda_i\}_{i=1}^M$ into Eqn. (14), we get the final adaptive regularization

$$\mathcal{A}(b) = \sum\nolimits_{i=1}^{M} \sqrt{k_i} \left| q_i^T b \right| \ . \tag{15}$$

In this work, Laplacian is adopted as the model distribution $q(b)$. In such case, the values $\{k_m\}_{m=1}^M$ in the diagonal matrix K satisfy that $k_m = 2(1 - \cos(\pi(m-1)/M)),\ m = 1, 2, \ldots, M$.

3. LEVEL SET FORMULATION

In this work, we consider the two-phase segmentation case[1], that is, $N = 2$. By using level set formulation, the segmentation likelihood energy can be rewritten as

$$\begin{aligned} \mathcal{L}(\phi, b) &= \gamma_1 \int_\Omega (I(\mathbf{x}) - b(\mathbf{x})c_1)^2 H_\varepsilon(\phi(\mathbf{x})) \mathrm{d}\mathbf{x} \\ &+ \gamma_2 \int_\Omega (I(\mathbf{x}) - b(\mathbf{x})c_2)^2 (1 - H_\varepsilon(\phi(\mathbf{x}))) \mathrm{d}\mathbf{x} \ , \end{aligned} \tag{16}$$

where $H_\varepsilon(x) = \frac{1}{2}\left(1 + \frac{2}{\pi}\arctan\left(\frac{x}{\varepsilon}\right)\right)$ is ε-Heaviside function, and its derivative is ε-Dirac function, given by $\delta_\varepsilon(x) = \frac{1}{\pi}\frac{\varepsilon}{\varepsilon^2 + x^2}$. As with the previous work, such as [8], the contour length regularization energy with level set formulation is

$$\mathcal{R}(\phi) = \int_\Omega |\nabla H_\varepsilon(\phi(\mathbf{x}))| \, \mathrm{d}\mathbf{x} \ . \tag{17}$$

Combining with Eqns. (15), (16) and (17), we can get the final objective energy functional:

$$\begin{aligned} \mathcal{F}(\phi, b, c) &= \gamma_1 \int_\Omega (I(\mathbf{x}) - b(\mathbf{x})c_1)^2 H_\varepsilon(\phi(\mathbf{x})) \mathrm{d}\mathbf{x} \\ &+ \gamma_2 \int_\Omega (I(\mathbf{x}) - b(\mathbf{x})c_2)^2 (1 - H_\varepsilon(\phi(\mathbf{x}))) \mathrm{d}\mathbf{x} \\ &+ \nu \int_\Omega |\nabla H_\varepsilon(\phi(\mathbf{x}))| \, \mathrm{d}\mathbf{x} + \mu \sum_{i=1}^{M} \sqrt{k_i} \left| q_i^T b \right| \ . \end{aligned} \tag{18}$$

[1] Same with [8], our model is easy to be extended to multi-phase case by introducing multiple level sets.

3.1. Optimization

The standard gradient descent method is used to minimize the energy functional Eqn. (18) by iterating following three steps.

Step 1 ($b, \phi \mapsto c$)**:** Keeping level set function ϕ and bias field b fixed, minimizing the energy functional $\mathcal{F}(\phi, b, c)$ with respect to c by variational method, given by

$$\begin{aligned} c_1 &= \frac{\int_\Omega I(\mathbf{x})b(\mathbf{x})H_\varepsilon(\phi(\mathbf{x}))\mathrm{d}\mathbf{x}}{\int_\Omega H_\varepsilon(\phi(\mathbf{x}))\mathrm{d}\mathbf{x}} , \\ c_2 &= \frac{\int_\Omega I(\mathbf{x})b(\mathbf{x})(1-H_\varepsilon(\phi(\mathbf{x})))\mathrm{d}\mathbf{x}}{\int_\Omega (1-H_\varepsilon(\phi(\mathbf{x})))\mathrm{d}\mathbf{x}} . \end{aligned} \tag{19}$$

Step 2 ($c, \phi \mapsto b$)**:** Keeping level set function ϕ, clusters c_1 and c_2 fixed, minimizing the energy functional $\mathcal{F}(\phi, b, c)$ with respect to b. Motivated by [12], it is solved by the following two sub-steps:

$$\text{finding } \Sigma^{-1}: \ \Lambda = K^{1/2}\text{diag}(Q^T b)^{-1}, \Sigma^{-1} = Q\Lambda Q^T , \tag{20}$$

$$\text{minimizing } b: \ \min_b \mathcal{L}(\phi, b) + \mu b^T \Sigma^{-1} b . \tag{21}$$

These two steps both have closed-form solutions. Unfortunately, it is very time-consuming to obtain the closed solution of the second minimizing step. In this work, we give a fast and approximate solution. Denote $\mathcal{E}(b) = \mathcal{L}(\phi, b) + \mu b^T \Sigma^{-1} b$, the solution is

$$0 = \frac{\partial \mathcal{E}(b)}{\partial b} = eb - f + \mu\Sigma^{-1} b , \tag{22}$$

where

$$\begin{aligned} e &= \gamma_1 c_1^2 H_\varepsilon(\phi) + \gamma_2 c_2^2 (1 - H_\varepsilon(\phi)) , \\ f &= \gamma_1 c_1 I H_\varepsilon(\phi) + \gamma_2 c_2 I (1 - H_\varepsilon(\phi)) . \end{aligned}$$

To facilitate presentation, we denote a diagonal matrix $E = \text{diag}(e)$. Hence, Eqn. (22) can be rewritten as

$$Eb + \mu\Sigma^{-1} b = f . \tag{23}$$

To solve Eqn. (23) fast, we ignore the term $\mu\Sigma^{-1} b$ first, and calculate $\tilde{b} = E^{-1} f$. Then, Eqn. (23) is approximate to

$$b - \tilde{b} + \mu E^{-1}\Sigma^{-1} b = 0 . \tag{24}$$

As presented in [12], Eqn. (24) can be solved fast by the following iterative function:

$$b^{t+1} = Q\frac{\text{diag}\left|Q^T b^t\right|}{\text{diag}\left|Q^T b^t\right| + \mu K} Q^T \tilde{b} , \tag{25}$$

in which the Q^T and Q are obtained by forward and inverse multi-dimensional DCT respectively.

Step 3 ($b, c \mapsto \phi$)**:** Keeping clusters c_1, c_2 and bias field b fixed, we minimize the objective functional $\mathcal{F}(\phi, b, c)$ with respect to ϕ, and obtain the following gradient descent flow:

$$\frac{\partial \phi}{\partial t} = -\delta_\varepsilon(\phi)\left(\gamma_1(I - bc_1)^2 - \gamma_2(I - bc_2)^2 - \nu\text{div}\left(\frac{\nabla\phi}{|\nabla\phi|}\right)\right) . \tag{26}$$

In Eqn. (26), the partial derivative is simply discretized as the central finite difference, and the temporal derivative as a forward difference.

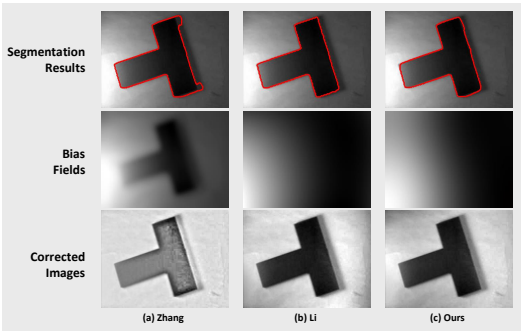

Fig. 1. Comparisons of our method with Zhang [7] and Li [9] on a synthetic image. (a) The results of Zhang's model. (b) The results of Li's model. (c) The results of our model.

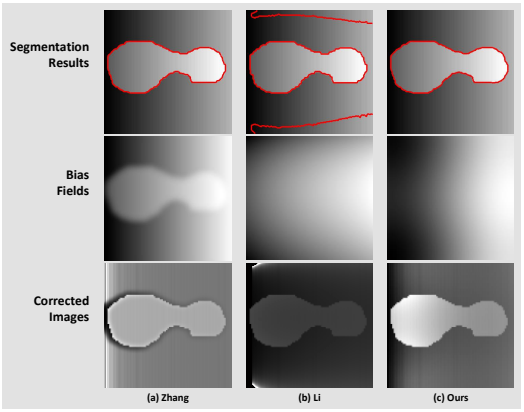

Fig. 2. Comparisons of our method with Zhang [7] and Li [9] on a synthetic image. (a) The results of Zhang's model. (b) The results of Li's model. (c) The results of our model.

3.2. Implementation

The main steps of the our algorithm is summarized as:

STEP_1. Initializing the level set function ϕ to be a binary function as follows:

$$\phi = \begin{cases} -\rho, & \mathbf{x} \in \Omega_{in} - \partial\Omega_{in} \\ 0, & \mathbf{x} \in \partial\Omega_{in} \\ \rho, & \mathbf{x} \in \Omega - \Omega_{in} \end{cases} , \tag{27}$$

where Ω_{in} is the inner of the initial contour $\mathcal{C}$, and $\partial\Omega_{in}$ is the boundary of Ω_{in}. Initializing the bias field b^0 as $b^0 = I \otimes g$, where g is the Gaussian kernel function.

STEP_2. Computing clusters c_1 and c_2 by Eqn. (19).

STEP_3. Computing the bias field b by Eqn. (25)

STEP_4. Evolving level set function ϕ by Eqn. (26).

STEP_5. Repeating **STEP_2**, **STEP_3** and **STEP_4** until ϕ and b converge or the maximum iteration number is reached.

4. EXPERIMENTS

In this section, we evaluate the proposed model by comparing it with two state-of-the-art approaches, namely, Zhang [7] and Li [9], on both synthetic and real images. All experiments are conducted in

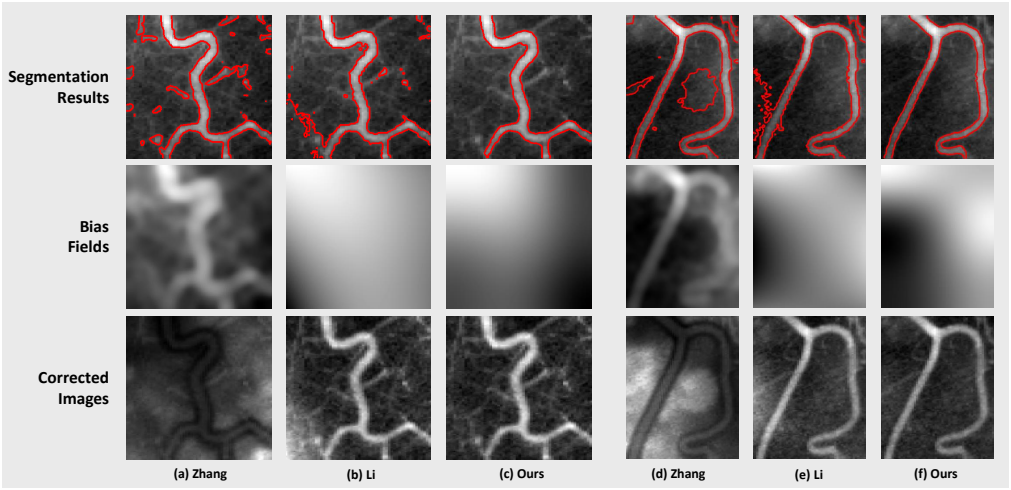

Fig. 3. Comparisons of our method with Zhang [7] and Li [9] on vessel images. (a) The results of Zhang's model. (b) The results of Li's model. (c) The results of our model. (d) The results of Zhang's model. (e) The results of Li's model. (f) The results of our model.

Matlab 7.0 programming environment on a 1.6 GHz Intel Pentium IV personal computer.

4.1. Synthetic Examples

Experimental results on a synthetic image are presented in Fig. 1. As shown in this figure, the results of the proposed method and Li's method look similar. Specifically, the bias fields estimated by these two methods are very smooth, and the corrected images are both homogeneous. However, Zhang's model produces an inaccurate segmentation result, and the estimated bias field by Zhang's model contains image structure information, which further causes an inaccurate bias correction result.

We evaluate our method on another synthetic image, in which the right part of background has higher intensities than the left part of object. As shown in Fig. 2, the segmentation results of our method and Zhang's method are similar, however, Li's method fails (see Fig. 2(b)). In Fig. 2(c), we can see that the bias field estimated by our method is more smooth, and the corrected image of our method is more homogeneous. As with Fig. 1, the estimated bias field of Zhang's method also has image structure information, which degrades the performance on the result of the corrected image (see Fig. 2(a) for details). In Fig.2 (b), we can see that the corrected image of Li's model is still hard to distinguish the target from background.

4.2. Real medical images

To further evaluate the performance of the proposed method, we apply the proposed model, as well as Li's and Zhang's to two real blood vessel images which present intensity inhomogeneity. As shown in Fig. 3, the segmentation results by our method (see Fig. 3(c) and (f)) are much more accurate than those by Zhang's (see Fig. 3(a) and (d)) and Li's (see Fig. 3(b) and (e)). It is worth noting that the bias fields estimated by our method are more smooth, and the corrected images are more homogeneous.

In Fig. 4, we show the results on a brain MR image by the above mentioned three models. As shown in Fig. 4(a) and (b), both Zhang's model and Li's model achieve almost the same segmentation results, which have better detailed information, but the bias fields estimated by their methods have image structure information, which leads to an inaccurate result on the corrected images. In our results (see Fig. 4(c)), the estimated bias field is smooth, and the corrected image is more homogeneous than the original one.

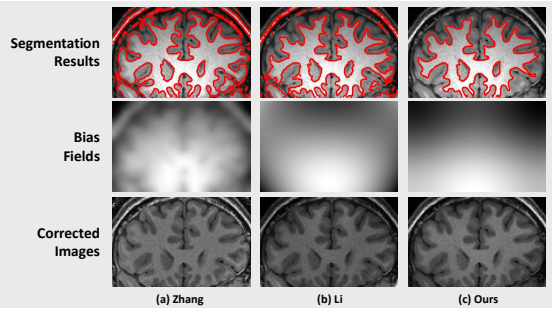

Fig. 4. Comparisons of our method with Zhang [7] and Li [9] on brain image. (a) The results of Zhang's model. (b) The results of Li's model. (c) The results of our model.

5. CONCLUSION

This paper presents a new level-set based segmentation approach to simultaneous bias correction and image segmentation for medical image. From a Bayesian perspective our method can make full use of the contour prior and the bias field prior. The smoothness of the bias field is intrinsically ensured by the adaptive regularization, which makes our estimated bias field more smooth and has less structural information of the original image. Comparisons with the other segmentation methods on synthetic and real medical images show that our method holds many advantages on the segmentation and bias field correction accuracies. In the future, we will extend our model by using multiple level set functions, and evaluate our model on more types of images.

6. REFERENCES

[1] David Rivest-Hénault and Mohamed Cheriet, "Unsupervised MRI segmentation of brain tissues using a local linear model and level set," *Magnetic Resonance Imaging*, vol. 29, no. 2, pp. 243–259, 2011.

[2] Xiuxia Xing, Youlong Zhou, Jonathan S. Adelstein, and Xinian Zuo, "Pde-based spatial smoothing: a practical demonstration of impacts on MRI brain extraction, tissue segmentation and registration," *Magnetic Resonance Imaging*, vol. 29, no. 5, pp. 731 – 738, 2011.

[3] Jainy Sachdeva, Vinod Kumar, Indra Gupta, Niranjan Khandelwal, and Chirag Kamal Ahuja, "A novel content-based active contour model for brain tumor segmentation," *Magnetic Resonance Imaging*, vol. 30, no. 5, pp. 694 – 715, 2012.

[4] Zujun Hou, "A review on MR image intensity inhomogeneity correction," *International Journal of Biomedical Imaging*, vol. 2006, pp. 1–11, 2006.

[5] U. Vovk, F. Pernus, and B. Likar, "A review of methods for correction of intensity inhomogeneity in MRI," *IEEE Transactions on Medical Imaging*, vol. 26, no. 3, pp. 405–421, 2007.

[6] Chunming Li, Rui Huang, Zhaohua Ding, J.C. Gatenby, D.N. Metaxas, and J.C. Gore, "A level set method for image segmentation in the presence of intensity inhomogeneities with application to MRI," *IEEE Transactions on Image Processing*, vol. 20, no. 7, pp. 2007–2016, 2011.

[7] Kaihua Zhang, Lei Zhang, and Su Zhang, "A variational multiphase level set approach to simultaneous segmentation and bias correction," in *IEEE International Conference on Image Processing*, 2010, pp. 4105–4108.

[8] Lingfeng Wang and Chunhong Pan, "Image-guided regularization level set evolution for MR image segmentation and bias field correction," *Magnetic Resonance Imaging*, vol. 32, no. 1, pp. 71 – 83, 2014.

[9] Chunming Li, John C. Gore, and Christos Davatzikos, "Multiplicative intrinsic component optimization (MICO) for MRI bias field estimation and tissue segmentation," *Magnetic Resonance Imaging*, vol. 32, no. 7, pp. 913 – 923, 2014.

[10] D. Cremers, S.J. Osher, and S. Soatto, "Kernel density estimation and intrinsic alignment for shape priors in level set segmentation," *International Journal of Computer Vision*, vol. 69, no. 3, pp. 335–351, 2006.

[11] Daniel Cremers, "Nonlinear dynamical shape priors for level set segmentation," *Journal of Scientific Computing*, vol. 35, no. 2-3, pp. 132–143, 2008.

[12] Andriy Myronenko and Xubo Song, "Adaptive regularization of ill-posed problems: Application to non-rigid image registration," *CoRR*, vol. abs/0906.3323, 2009.